LBL-8501

Lawrence Berkeley Laboratory
UNIVERSITY OF CALIFORNIA

Materials & Molecular
Research Division

AN INVESTIGATION OF THE EFFECTS OF PARTICLE SIZE ON THE MECHANICAL PROPERTIES OF POROUS AND TIN INFILTRATED NIOBIUM RODS FABRICATED BY A THERMOPLASTIC-POWDER METALLURGY TECHNIQUE

Abid Noman
(M. S. thesis)

December 1978

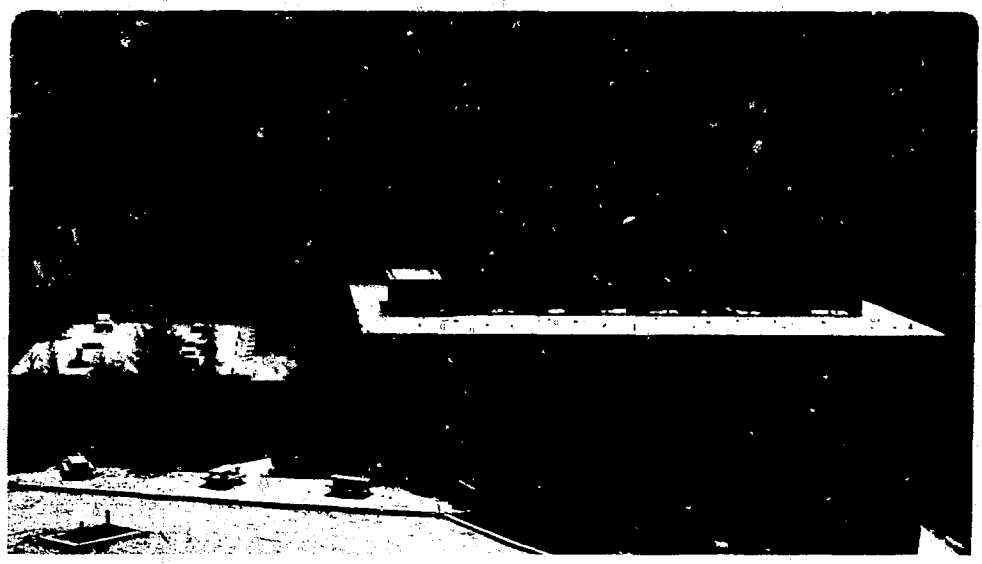

Prepared for the U.S. Department of Energy under Contract W-7405-ENG-48

TABLE OF CONTENTS

AN INVESTIGATION OF THE EFFECTS OF PARTICLE SIZE ON THE MECHANICAL PROPERTIES OF POROUS AND TIN INFILTRATED NIOBIUM RODS FABRICATED BY A THERMOPLASTIC-POWDER METALLURGY TECHNIQUE

Abid Noman

Materials and Molecular Research Division
Lawrence Berkeley Laboratory, University of California,
Berkeley, California 94720

ABSTRACT

An investigation was made of the influence of particle size on the properties of both porous and tin infiltrated niobium rods fabricated by a thermoplastic-powder metallurgy technique. The residual porosity, extrusion pressure, tensile strength and ductility were found to be dependent on the particle size distribution. All of these parameters were found to increase with increasing particle size. The influence of sintering time at a temperature of 2250°C was also studied. With increasing sintering time, the residual porosity and tensile strength decreased, whereas the ductility increased.

The procedures for fabricating infiltrated niobium rods and the various tests employed to determine their properties are described.

I. INTRODUCTION

Since the advent of the industrial revolution, the consumption of fossil fuels increased markedly. With subsequent innovations and changes in the state of technology, this consumption increased from a linear to an exponential rate. Today, a threat is posed on the depletion of this finite resource, thus compelling the scientists to investigate methods, primarily to find new means of generating energy and secondarily to preserve the available energy.

High field superconductivity comes into the picture as an alternative for generating and conserving energy. It is being used in socially beneficial areas such as mass transit systems for levitating and propelling trains, transmission of electric power with minimal loss, as well as in devices such as advanced computers, gyro devices, large superconductive particle accelerators and for magnetic fusion.

The phenomenon of superconductivity was discovered by H. Kamerling Onnes[1] in 1911. Onnes, who was the first to liquify helium, found that mercury suddenly lost all electrical resistance at 4.1°K; that is, it became a perfect conductor. This phenomenon was termed superconductivity. In the following years little progress was made because no known superconductors had practical application until the early 1960's when Kunzler *et al*[2] discovered that Nb_3Sn remained superconductive in high magnetic fields. Envisioning the extreme usefulness of superconducting materials, tremendous efforts are being made in the research and development of these superconducting materials and devices today. Some prototype quasi-commercial devices are already

in use and approximately 30 million dollars are being spent annually to further develop this technology.[3]

The research and development of superconducting materials is generally broken into two categories:

1. Materials which can be fabricated by conventional metal working processes. An example would be ductile solid-solution alloys, such as those of niobium and titanium.

2. A15, intermetallic compounds such as Nb_3Sn, $Nb_3(Al,Ge)$ and $Nb_3(Al,Si)$ which are very brittle and require special fabrication techniques. The A15 compounds exhibit superior critical magnetic fields and critical temperatures which allows the use of liquid hydrogen rather than liquid helium to cool the superconductor, which in turn adds to the feasibility of using compounds of this type commercially.

Presently the method being employed commercially is the "Bronze Process."[4] This process has its advantages as well as drawbacks. The main advantage is the inherent stability imparted to the wire as a result of its multifilamentary structure. This process has been used to produce Nb_3Sn and V_3Ga composite superconductors. On the other hand, the Bronze Process lacks versatility, insofar as the extension of the process to a variety of materials is concerned. For example, the Bronze Process has been found to be ineffective for aluminum-containing compounds, which exhibit good superconducting properties.

An alternate method has been developed at the Lawrence Berkeley Laboratory for the fabrication of superconducting materials, employing a powder metallurgy-infiltration technique. This technique has been successfully extended to the Nb_3Sn[5], Nb_3Al[6], $Nb_3(Al,Ge)$[7] and $Nb_3(Al,Si)$[8]

systems. For the fabrication of niobium rods, which are prepared from powder and are to be infiltrated at a later stage, two methods have been employed successfully. The first technique makes use of isostatic compaction[9] and the second method employs as a binder a polymer, which is coated on the powder particles, thus rendering to the powder thermoplastic properties.[10] Taking advantage of the thermoplastic properties of the powder, the substance is extruded as a rod, after which the polymer is volatilized by means of a prescribed heating cycle. It remains to expose the niobium rod obtained after initial sintering to a final stage, high temperature sintering to impart the final strength and ductility and to facilitate the removal of oxide layer which hampers the infiltration of the rod. The feasibility of this process for producing and infiltrating niobium rods was shown by Nordin.[11] To obtain a superconducting wire from infiltrated rods, a mechanical reduction to obtain the wire, and an additional heat treatment for the formation of the A15 superconducting phase[12] are necessary.

This investigation employs the thermoplastic-powder metallurgy technique and reports the effects on mechanical properties, as well as on the process parameters, of three different particle size ranges and sintering time.

II. EXPERIMENTAL METHODS

It required five steps to go from niobium powder to infiltrated niobium rods. To obtain tensile specimens an additional machining step was introduced after infiltration. These five steps were:

1. Coating of niobium powder with a polymer, thus imparting to it thermoplastic properties.

2. Extrusion of niobium-plastic mixture to obtain rods.

3. First stage sintering, which was a prescribed heating cycle to volatilize the polymer and impart handling strength to the niobium rods.

4. High temperature sintering to impart the final strength, porosity and ductility to the niobium rods and to effect the removal of oxide layer and other contaminants, which could hamper infiltration.

5. Infiltration of the rods with tin to fill the network of interconnected pores.

The process is shown schematically in Fig. 1.

A. The Process

1. Coating of powder (The uncoated powder is shown in Fig. 2) -

To impart thermoplastic properties, the powder was coated with a polymer. The polymer chosen was polystyrene. Selection of polystyrene was based on the fact that the oxide and contaminating residues deposited on the niobium particles after volatilization are minimal.[13] The amount of polymer added to the powder was treated as a fixed parameter in this investigation. After several trial extrusions extruded rods favorable properties: that is, a fine surface finish as well as reasonable pore size and residual porosity. Lesser amounts of polystyrene would

give a rough surface to the extruded rods and too high an amount of polystyrene would give too high a residual porosity. To facilitate the additon of polystyrene to the powder a 3% solution (by weight) of polystyrene in toluene was prepared. Polystyrene is not readily soluble in toluene; the mixture was therefore left for about twenty-four hours, after which it was stirred briskly and a solution obtained. An amount of this solution was added to niobium powder placed in a pyrex dish to give 8% polystyrene fraction by weight. To coat the niobium particles with polystyrene, the mixture was slowly heated on a hot-plate to evaporate the toluene. During the heating operation extra care was taken in continuously stirring the mixture, as the quality of extruded rods was strongly dependent on how well the powder was coated, which in turn was controlled by good mixing, implying gentle but thorough stirring.

When most of the toluene had evaporated a desired amount of plasticizer, which was 1/5 the weight of polystyrene, was added to the mixture. This plasticizer (27% diphenyl and 73% diphenyl ether) effectively decreases the required extrusion pressure. After a short while of continued heating the mixture became rubbery in consistency, making further stirring ineffective. The niobium powder was now coated with polystyrene, and to remove the final traces of toluene, the mixture was placed in an oven and heated for one hour at 115°C. The substance was hard at this stage and had to be cut in small pieces to effectively fit the extrusion cylinder. It was observed that best results were obtained when the pieces of niobium-plastic mixture were small.

2. Extrusion -

The extrusion was done by means of a hand-operated hydraulic press. The apparatus used for extrusion is shown in Figure 3. The maximum achievable fluid pressure in the hydraulic press was 3000 pounds; the diameter of the loading ram was three inches, whereas the diameter of the extrusion cylinder was one inch. Therefore, the maximum extrusion pressure available was 27,000 psi.

Bits of niobium-plastic were placed in the extrusion cylinder, which was pre-heated to 165°C by means of a cylindrical heating element. The apparatus was so arranged that below the bits of niobium-plastic mixture was the extrusion die, below which was a base plug with a central hole, which in turn rested on an asbestos ring as a measure to prevent it from acting as a heat sink. The material was allowed to attain a steady temperature of 165°C. It was found that fifteen to twenty minutes were necessary for that purpose. Next, pressure was applied. The pressure increased until the material started extruding, after which it remained constant until all the material had been extruded. The extruded rod was allowed to cool while hanging from the apparatus for a few minutes and then broken off. The extruded rods varied from 14 to 16 inches in length and were 3/16 inch in diameter (Figure 4).

3. First stage sintering -

The purpose of first stage sintering was to volatilize the polystyrene as well as impart handling strength to the niobium rods. This was achieved by exposing the niobium-plastic rods to a prescribed heating cycle. The heating cycle was as follows: Ambient temperature to 400°C in approximately one hour; held at 400°C for one hour to

vaporize the polystyrene; 400°C to 1300°C in 45 minutes to one hour; sintered at 1300°C for one hour to impart the handling strength to the rods.

The first stage sintering was conducted in a horizontal mullite tube furnace as shown in Figure 5. The heating was carried out in an inert atmosphere of argon and inert gas was circulated through the tube to carry away the contaminating vapors to a series of oil baths. Passing the vapors through oil baths reduced the pollution of the laboratory. The size of the hot zone, about 13 cms. (5 inches), restricted the length of the rods which were to be sintered. At some point during the heating cycle the rods lack strength enough to support their own weight, which dictated that the rods be supported during sintering. The support used was a tee-shaped tantalum trough. After being exposed to the prescribed heating cycle, the rods appeared straight and smooth as shown in Figures 6 and 7, with strength enough to withstand handling stresses.

4. Final stage (high temperature) sintering -

The purpose of high temperature sintering was to impart to the niobium rods the final strength and ductility and to remove oxide layers and other contaminants deposited on the niobium particles. This operation was conducted in an Abar furnace (Fig. 8) the length of the niobium rods sintered at this stage was dictated by the length of the hot zone (about 6.5 cms. or 2.5 inches). The rods of niobium were hung vertically in the hot zone by means of a tantalum wire, which was attached to a tantalum rod (Fig. 8) at the other end.

The samples were heated to a temperature of 2250°C at a pressure of 10^{-6} mm Hg for varying times.

5. Infiltration -

Infiltration of the niobium rods with tin was done immediately after the high temperature sintering. A tin bath was contained in a graphite crucible which was placed in a quartz tube (Fig. 8) and heated to a temperature of 600°C. After the niobium rod had been sintered for the desired time, the temperature of the furnace was turned down to 600°C and enough time allowed for the rod to attain the same temperature as the tin bath. The niobium rod was then lowered into the tin bath until it was completely immersed. Next the pressure was increased from 10^{-6} mm Hg to a little below atmospheric pressure to force the tin into the pores. The infiltration time was 1 1/2 minutes.

To prepare tensile specimens of porous or tin infiltrated niobium rods, the rods were straightened and then machined on a lathe. The niobium rods were 3/16 inch in diameter and 2 1/4 inches in length, whereas the tensile specimens had a grip on each end which was 0.54 inches long and 3/16 inch in diameter and the test section was 1.25 inches long and 1/10 inch in diameter.

B. Analytical Techniques Employed

Optical microscopy was employed, to confirm that the infiltration of the sintered niobium rods with tin was complete, and to ascertain if the infiltrated tin had reacted with the niobium matrix.

An anodization method developed by Picklesimer[14] was used to distinguish the constituency of as-infiltrated niobium rods. It gave a characteristic color to each phase: blue for niobium, yellow for tin and reddish brown for Nb_6Sn_5.

The porosity of the niobium rods was determined, after the final sintering, by sealing the pores of the rod with epoxy resin and weighing the rod in water to determine the buoyant force and hence its volume. By knowing the density of niobium and weight of sample, the porosity of niobium rods was calculated:

$$\text{Porosity} = \frac{\text{Vol (pores)}}{\text{Vol (total)}}$$

$$= \frac{\text{Vol (total)} - \text{Vol (Nb)}}{\text{Vol (total)}}$$

$$= 1 - \frac{\text{Vol (Nb)}}{\text{Vol (total)}}$$

where, Vol (total) is the volume of Nb rod, calculated from the buoyant force and $\text{Vol (Nb)} = \frac{\text{Weight of Nb rod}}{\text{Density of Nb}}$.

An Instron machine was used to perform mechanical tests on the porous and tin infiltrated niobium rods. These tests were performed on specimens made from three different particle size powders with the sintering time varying from 5 to 20 minutes.

Scanning Electron Microscopy (SEM) was used to determine the mode of fracture on the surface of fractured specimens.

An attempt was made to separate the as-received powder into different groups, according to the particle size distribution, by using a Powder Micro-Classifier. This attempt failed as the Micro-Classifier would only separate the very fine part, i.e., the dust present in the as-received powder.

the range -325 +400 mesh. The extrusion was a failure as shown in Fig. 9. Next the plastic content was raised to 10% by weight and an extrusion attempted. Again the extrusion failed (Fig. 10). It seemed as though the particles were not coated adequately with plastic and it was observed that just before the substance began to flow through the extrusion die a moderate amount of polystyrene seeped through the niobium-plastic mixture and out of the extrusion die. It was surmised that fine particles are essential for a successful extrusion to trap the plastic inside the mixture which can otherwise seep out. To confirm this, an extrusion was attempted with 80%, -325 +400 mesh particles and 20%, -1.5 +.5 mesh particles by weight. This extrusion was successful with normal extrusion pressure and surface finish. However, time was not available to make an in depth analysis of the composition of the optimum blend necessary for successful extrusions. The variation of extrusion pressure with particle size is shown in Fig. 11. The finer particle grain extrudes at a lower pressure due to the homogeneity of the substance and because the finer particle-plastic mixture flows with relative ease through the extrusion die.

During the first stage sintering it was necessary to have the mullite tube well sealed. Even a small leak would allow air flow, which resulted in a partial oxidation of the niobium rod being sintered. It was also required to place the plastic-niobium rod right in the middle of the hot zone. If this practice was not followed, some of the vaporized plastic would deposit on the cooler parts of the rod, thus fouling it. It was essential to have a nice, clean rod (Figs. 12 and 13) for the high temperature (final stage) sintering as the

Abar furnace was extremely sensitive to contaminants. During the final sintering extreme caution was taken in hanging the niobium rods in the hot zone. This caution stemmed from the fact that the rods to be sintered were 2 1/4 inches long, whereas the hot zone was only slightly longer than 2 1/4 inches.

The plot for residual porosity versus time is shown in Fig. 14. This confirms what was expected. Larger particles with greater surface area form a more porous body than particles of smaller size. The porosity decreases with sintering time as the bonding of particles causes the pores to shrink. The pore size as shown in Fig. 15 decreases progressively from the relatively coarse to finer particle groups.

Although optimization of the infiltration temperature was not made, several infiltrations were tried at 575°C, 600°C and 625°C. The samples infiltrated at 575°C and immersed in the tin bath for 1 1.2 minutes showed voids which had not been infiltrated. At 625°C, there was a definite reaction between the niobium matrix and tin, resulting in the formation of Nb_6Sn_5, which is a brittle intermetallic compound. At 600°C the tin did not react with the niobium matrix at all and all the voids seemed to be filled after 1 1.2 minutes of immersion. Figures 16 and 17 shown the microstructure of various infiltrated rods.

The tensile tests conducted showed:

1) The relatively coarse particle rods sintered for the same length of time as finer particle rods, porous or infiltrated, were stronger than the respective finer particle rods (Figs. 18, 19, and

20). This was presumably due to the lower surface to volume ratio of the coarser particles, which implies that less contaminants were present in the coarser particle rods resulting in greater strength.

2) Coarse particle rods were more ductile than the respective finer particle rods (Figs. 21 and 22). This was again due to the fact that coarse particle rods had less contaminants due to the lower surface to volume ratio.

3) The tensile strength of the infiltrated rods decreased with sintering time (Figs. 19 and 20); this was presumably due to the grain growth and migration of contaminants to the boundaries.

4) Infiltrated rods were stronger than the respective porous rods; this was due to filling of the pores which provided the infiltrated rods with greater strength (Fig. 23).

5) Infiltrated rods made from fine particles were more ductile than the respective porous rods (Fig. 24). The difference decreased markedly for rods made from coarser particles.

6) Elongation of all the infiltrated rods increased with sintering time (Fig. 22). This would be expected as the oxide layer and contaminants are removed due to sintering, thus rendering the rods softer or more ductile.

The surface of fracture for various porous and tin infiltrated rods is shown in Figs. 25, 26 and 27. A comparison between Figs. 25 and 26, 27 indicates the relatively low ductility of the porous rods. In Fig. 25(b) the faint lines depict the bonding mechanism of particles due to sintering. Fig. 26 shows fractured surface of tin infiltrated, relatively fine [5-10 μ, Fig. 26(a)] and coarse [20-53 μ, Fig. 26(b)],

niobium rods, the sintering time being five minutes. At this high magnification some voids are visible, which normally would not be if the usual optical magnification (160x) were used. These voids cannot be seen in Fig. 27, where the sintering time is increased to 15 minutes, implying a more complete infiltration at higher sintering times, probably due to the removal of oxide layers and other contaminants. The fractured surface of the tin infiltrated specimens seems quite ductile, which confirms the quantitative results obtained.

IV. CONCLUSIONS

1. The process is feasible not only for fine particles (-400 mesh) as reported earlier by Nordin,[15] but also for coarser particles (as-received -270 mesh). However, for a successful extrusion of -270 mesh particles, the coating process has to be conducted with due care and caution.

2. In his report, Nordin ascertained that the residual porosity of niobium rods could be affected by controlling the amount of plastic added to the powder. Now, as an alternative, the residual porosity can be controlled by varying the size of the powder particles being used.

3. For the formation of A15 compound, the ideal residual porosity of niobium rods is 20-25%. From the plot for residual porosity versus sintering time for different particle size rods (Fig. 14), it is obvious that rods prepared from coarser particles will not contain the desired porosity. The fine particle rods would give the required porosity for 6.5 to 9.5 minutes of sintering time, whereas the medium particle rods seem to be most versatile, in that the desired porosity can be obtained for 9.5 to 20 minutes of sintering time. Two measures can be taken to effectively reduce the porosity of the rods prepared from coarser particles to a desirable level, as these rods exhibit the best ductility, a property of great significance for wire drawing:

a) By increasing the sintering time (increasing the sintering temperature would be another alternative, but is not feasible due to the limited power of the furnace).

b) By blending a fraction of fine particle size range with the relatively coarse particles.

These two measures mentioned above are quite involved and a detailed study was not within the scope of the investigation.

4. The optimum infiltration temperature obtained was 600°C. At this temperature, the pores were completely filled, with no observable reaction between the niobium matrix and tin. The infiltration time allowed at 600°C was 1 1/2 minutes.

5. As can be seen from the plots for tensile strength and ductility versus sintering time, the tensile strength decreases whereas the ductility increases with sintering time. From experience, it has been determined that in wire drawing the ductility plays a more important role than tensile strength. It is, therefore, desirable to have rods with the highest possible ductility (7.1% for fine particle rods after 7.5 minutes of sintering and 9.2% for medium particle rods after 20 minutes of sintering).

6. The extrusion failure of -325 +400 mesh particles indicates that a certain fraction of fine particles along with a coarser fraction is necessary for a successful extrusion. It might be of interest to optimize the fraction of fine particles of a certain particle range that would be required for successful extrusions.

ACKNOWLEDGMENT

This work was supported by the Division of Materials Sciences, Office of Basic Energy Sciences, U.S. Department of Energy.

The author wishes to thank Prof. Milton R. Pickus for guidance, valuable comments and suggestions throughout the research project. Discussions with Dr. John Ling-Fai Wang were extremely enlightening and productive and were greatly appreciated.

Thanks are also due to J. T. Holthuis for his technical assistance, J. A. Jacobsen for his assistance in metallographic techniques, and colleagues, Mr. Binh Phung, Mr. Chris Rutan and Mr. Tim Lam, whose presence was intellectually stimulating.

REFERENCES

1. H. K. Onnes, Comm. Phys. Lab., University of Leiden, 119, 120, 122, 1911.

2. J. E. Kunzler, E. Bueler, F. S. L. Hsu and J. H. Wernick, Phys. Rev. Letters, 6, 89 (1961).

3. B. Schwartz and S. Foner, Physics Today, 34., July, 1977.

4. M. Suenaga, W. B. Sampson, D. K. Klamut, IEEE Trans. Mag -11, 657, 1975.

5. K. Hemachalam, M. R. Pickus., J. Less Common Metals, 46, 29, 1976.

6. Thomas Tom, M.S. Thesis, LBL-188, 1971.

7. M. R. Pickus, M. P. Dariel, J. T. Holthuis, J. Ling-Fai Wang and J. Granda, Applied Physics Letters, 29, No. 12, 810, 1976.

8. Gary C. Quinn, M.S. Thesis, LBL-6999, 1977.

9. M. R. Pickus, J. Ling-Fai Wang, Modern Developments in Powder Metallurgy, 11, 315, 1977.

10. M. R. Pickus, Tips for Fountain Pens - A Case History on the Adaptability of the Powder Metallurgy Process, Int. Journal of Powder Metallurgy, 5 (3), 1969.

11. Dennis R. Nordin, M. S. Thesis, LBL-7346, 1978.

12. Ibid, Reference 9.

13. M. R. Pickus, M. Wells, A Technique for Extrusion Forming of Brittle and Refractory Compositions, Powder Metallurgy, Vo. 8, No. 16, 1965.

14. M. L. Picklesimer, U.S.A.E.C., Oak Ridge National Laboratory, Report 2296, 1957.

15. Ibid, Reference 11.

FIGURE CAPTIONS

Fig. 1. Schematic diagram of the infiltrated rod fabricating process.

Fig. 2. Photograph of different particle size groups used in the investigation

a) 5 - 10 μ (-1250 + 2500 mesh)

b) 10 - 20 μ (-625 + 1250 mesh)

c) 20 - 53 μ (-270 + 625 mesh)

Fig. 3. Photograph of the extrusion apparatus. From left to right: heater, plunger with thermocouple well drilled in the center; extrusion cylinder; extrusion die; base plug with a central hole.

Fig. 4. Photograph of a typical as-extruded niobium-plastic rod.

Fig. 5. Schematic diagram of the mullite tube furnace used for the removal of polystyrene and first stage sintering.

Fig. 6. Photograph showing a contrast between an as-extruded Nb-plastic rod and Nb rod after first stage sintering (5 - 10μ particle range).

Fig. 7. Photograph showing a contrast between an as-extruded Nb-plastic rod and Nb rod after first stage sintering (20 - 53μ particle range).

Fig. 8. Schematic diagram of Abar furnace:

1) extension tube; 2) tantalum rod; 3) back filling port; 4) electrical leads; 5) heating element; 6) niobium specimen; 7) radiation shields; 8) water-cooled walls; 9) W-5% Re vs. W-26% Re thermocouple junction; 10) vacuum connection; 11) quartz tube; 12) graphite crucible; 13) liquid tin and 14) resistance heater.

Fig. 9. Photograph of an extrusion failure with particle size group -325 +400 mesh and 8% polystyrene by weight.

Fig. 10. Photograph of another extrusion failure with particle size group -325 +400 mesh and 10% polystyrene by weight.

Fig. 11. Plot for extrusion pressure vs. particle size group.

Fig. 12. Photograph of Nb-rod after first stage sintering (5 - 10 μ particle range).

Fig. 13. Photograph of Nb rod after first stage sintering (20 - 53 μ particle range).

Fig. 14. Plot for residual porosity vs. sintering time.

Fig. 15. Micrographs of Nb rods infiltrated with epoxy after 15 minutes of high temperature (2250°C) sintering. Dark areas are epoxy resin while light areas are Nb.

a) 5 - 10 μ particle range

b) 10 - 20 μ particle range

c) 20 - 53 μ particle range

Fig. 16. Micrographs of tin infiltrated Nb 5 - 10μ range rods, sintered for 15 minutes at 2250°C.

a) Tin infiltration done at 600°C for 1 1/2 minutes with the Nb rod pre-heated to 600°C (unreacted).

b) Tin infiltration done at 625°C for 1 1/2 minutes with the Nb rod pre-heated to 625°C (reacted, with Nb_6Sn_5 formation).

Fig. 17. Micrographs of tin infiltrated Nb rod, sintered for 15 minutes at 2250°C. Tin infiltration done at 600°C for 1 1/2 minutes with the Nb rod preheated to 600°C.

a) 10 - 20 μ particle range rod (unreacted).

b) 20 - 53 μ particle range rod (unreacted).

Fig. 18. Plot for yield and ultimate strength vs. particle size for porous Nb rods.

Fig. 19. Plot for yield strength vs. sintering time for as-infiltrated Nb rods.

Fig. 20. Plot for ultimate strength vs. sintering time for as-infiltrated Nb rods.

Fig. 21. Plot for per cent elongation and per cent reduction in area vs. particle size for porous Nb rods.

Fig. 22. Plot for per cent elongation vs. sintering time for as-infiltrated Nb rods.

Fig. 23. Comparison of yield and ultimate strength of respective porous and as-infiltrated Nb rods.

Fig. 24. Comparison of elongation of respective porous and as-infiltrated Nb rods.

Fig. 25. SEM micrograph of fractured surface of porous Nb rods sintered at 2250°C for 15 minutes.

a) 5 - 10 μ particle range specimen

b) 10 - 20 μ particle range specimen

c) 20 - 53 μ particle range specimen

Fig. 26. SEM micrograph of fractured surface of as-infiltrated Nb rods.

a) 5 - 10 μ particle range, sintered for 5 minutes at 2250°C before infiltration at 600°C.

b) 20 - 53 μ particle range, sintered for 5 minutes at 2250°C before infiltration at 600°C.

Fig. 27. SEM micrograph of fractured surface of as-infiltrated Nb rods.

a) 5 - 10 μ particle range, sintered for 15 minutes at 2250°C before infiltration at 600°C.

b) 10 - 20 μ particle range, sintered for 15 minutes at 2250°C before infiltration at 600°C.

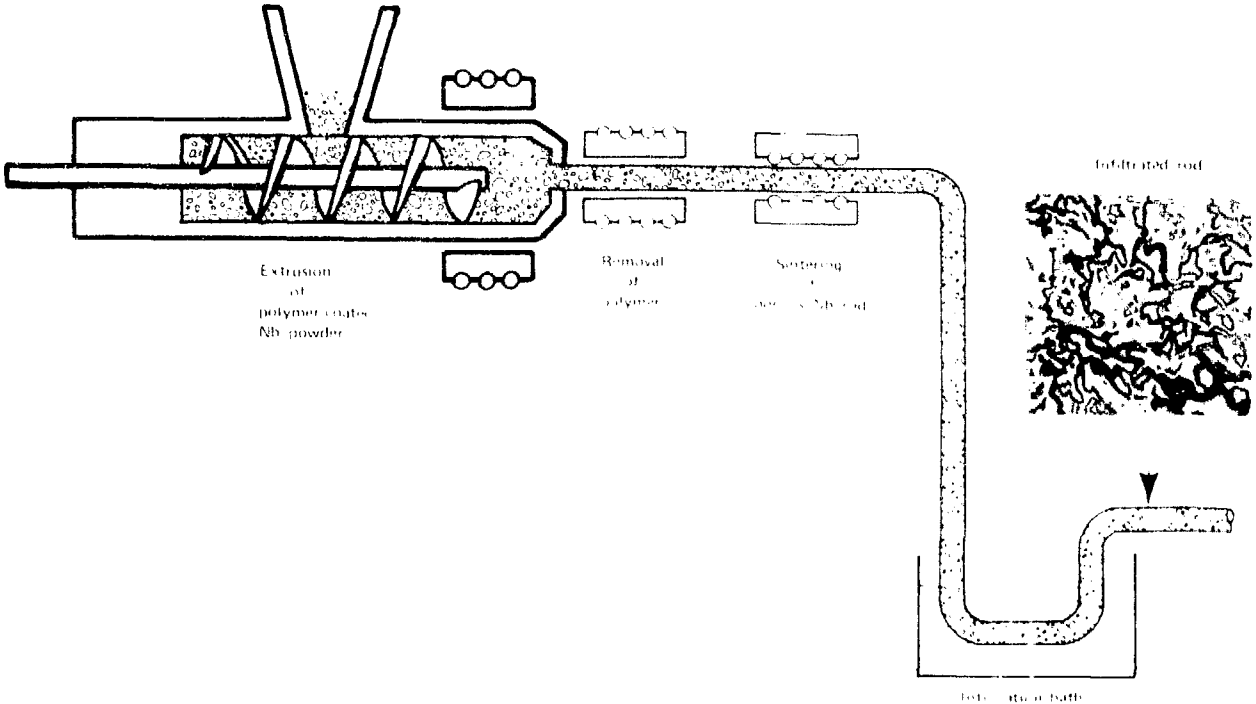

A CONTINUOUS PROCESS FOR
PRODUCING INFILTRATED Nb ROD FOR FABRICATING MULTIFILAMENTARY SUPERCONDUCTING

Fig. 1.

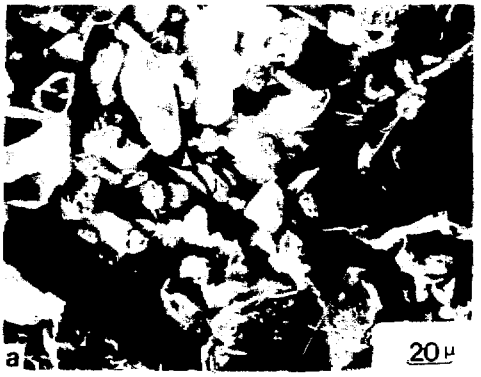
a
20μ


b
20μ


c
20μ

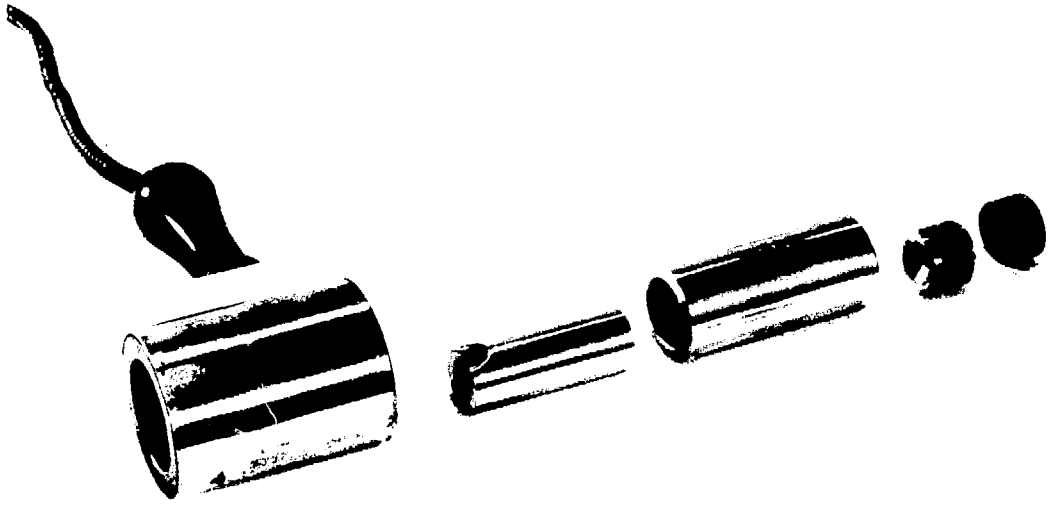

Fig. 3.

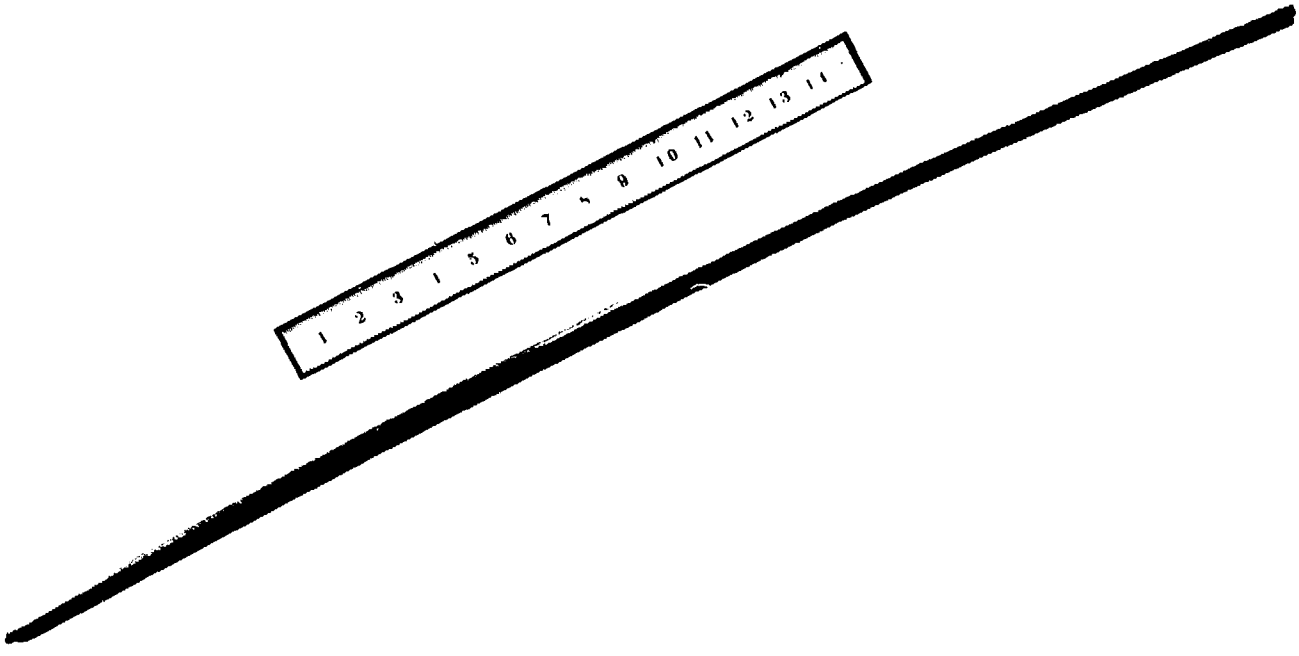

Fig. 4.

XBB 785-6642

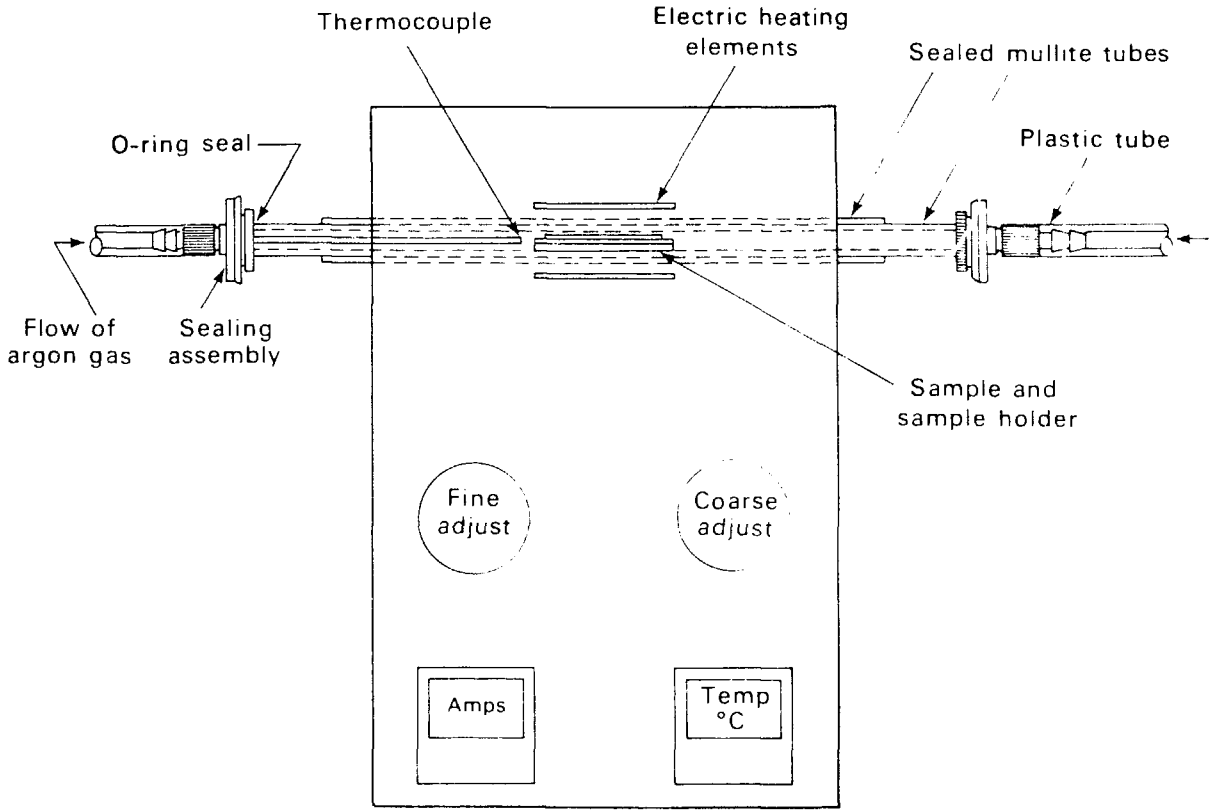

XBL 781-4

Fig. 5.

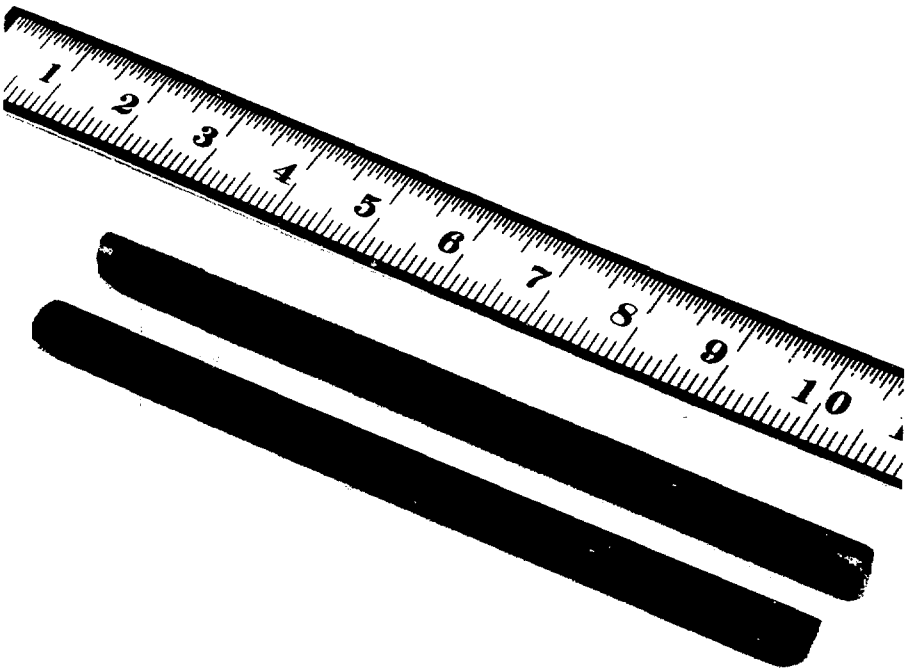

BBC 787-8332

Fig. 6.

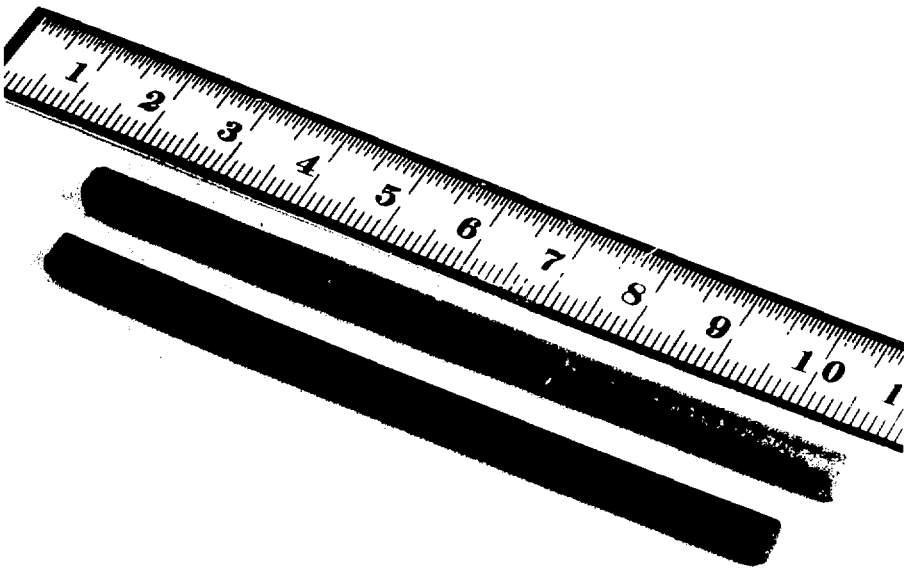

BBC 787-8330

Fig. 7.

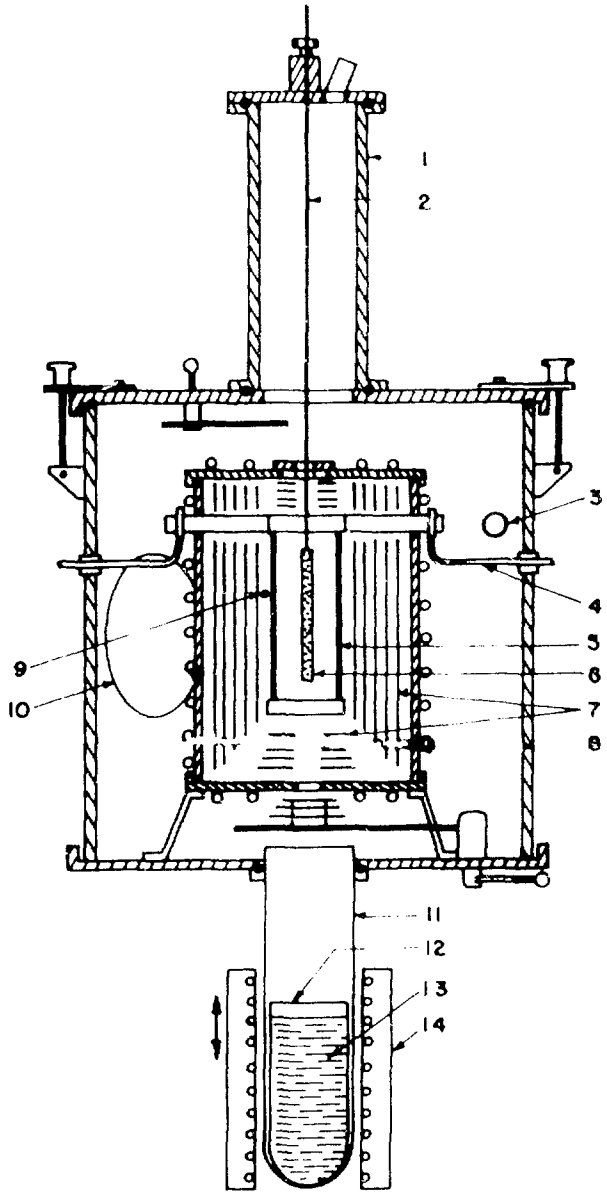

Fig. 8.

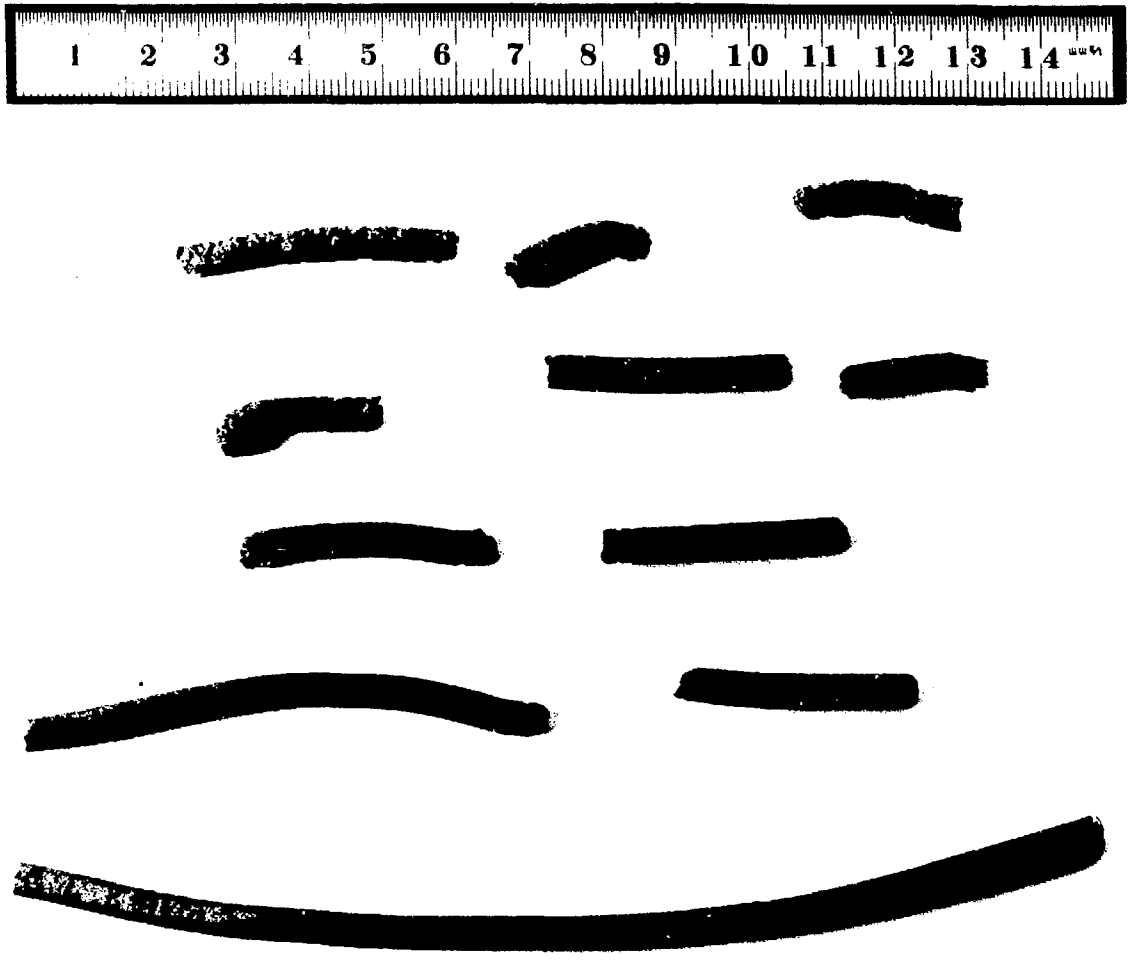

Fig. 9.

XBB 785-6646

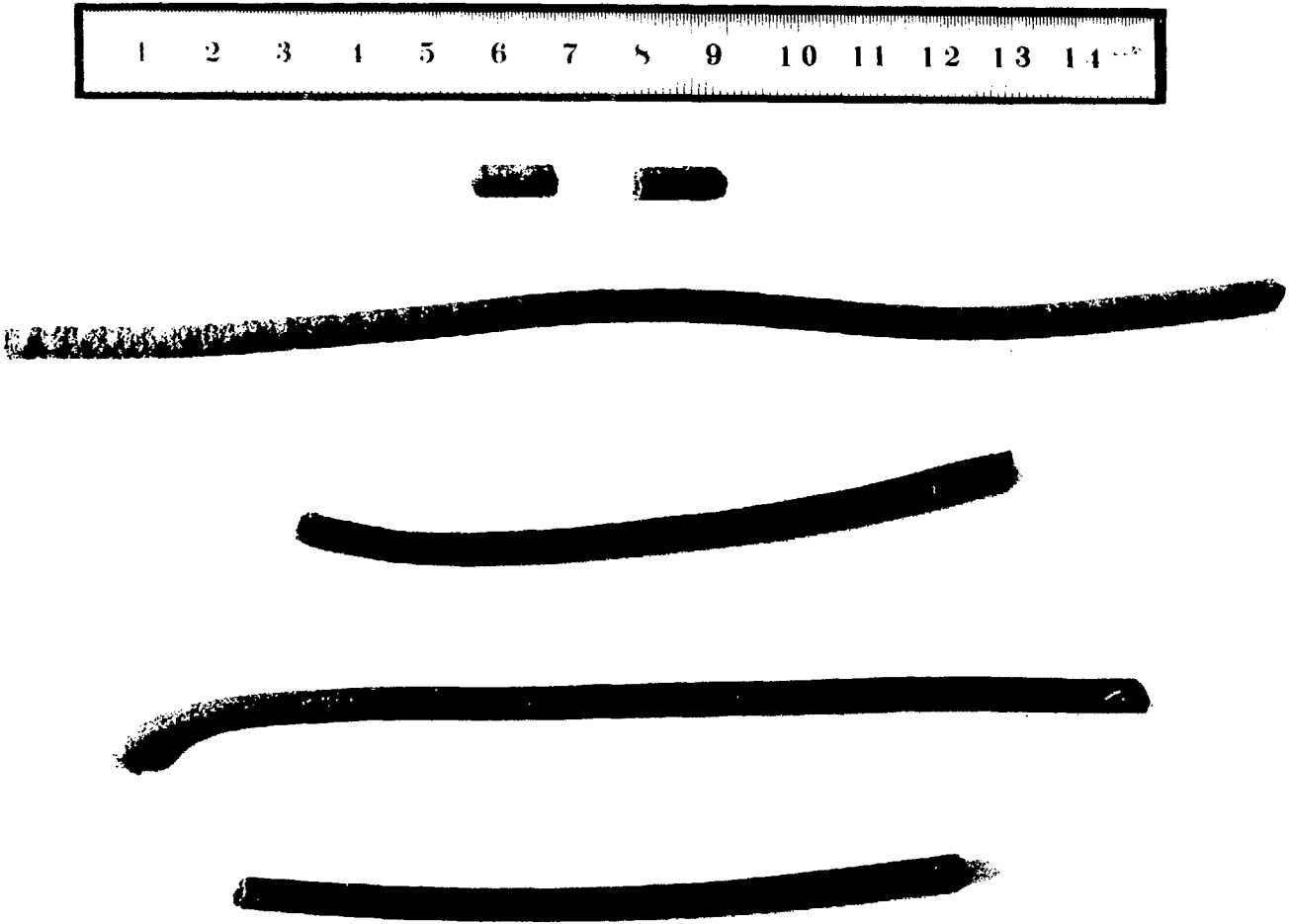

XBB 785-6645

Fig. 10.

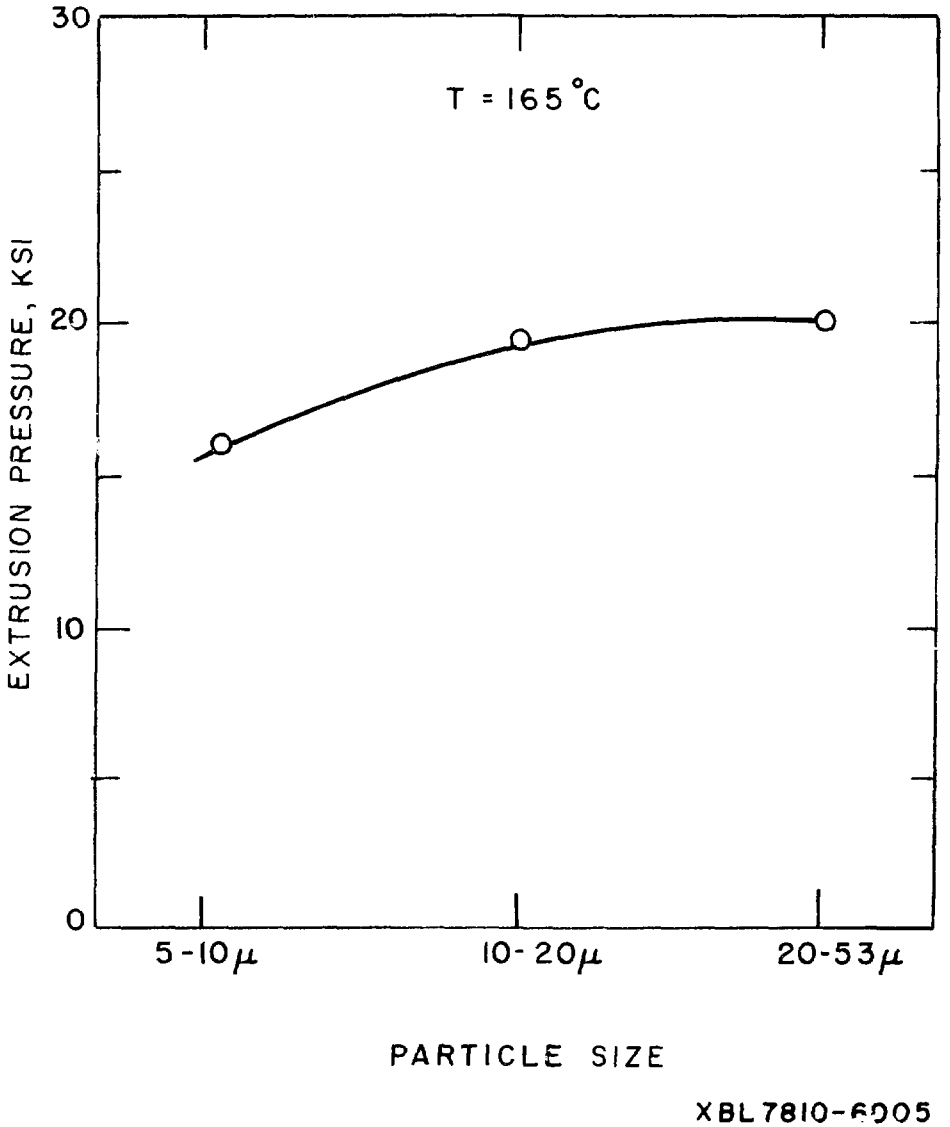
30
20
10
0
T = 165 °C
EXTRUSION PRESSURE, KSI
5-10μ
10-20μ
20-53μ
PARTICLE SIZE
XBL7810-6005

Fig. 11.

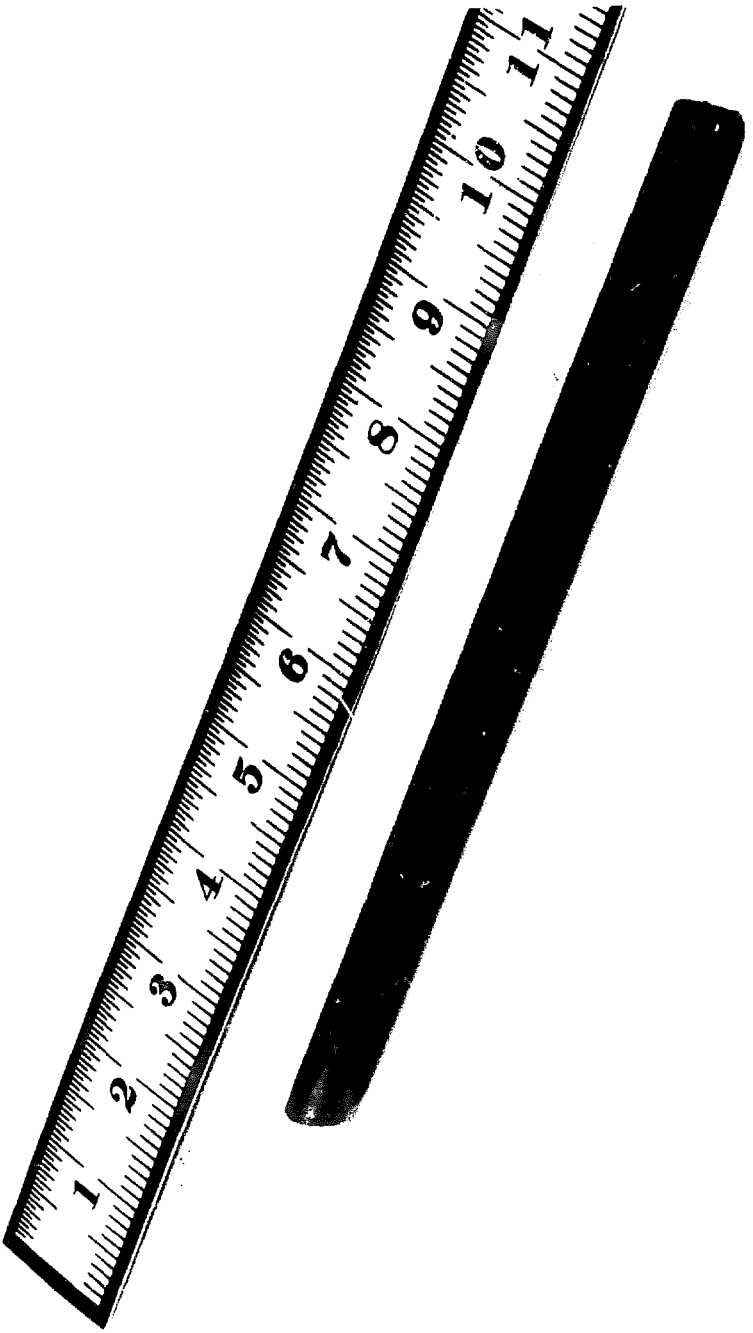

XBB 785-8333

Fig. 12.

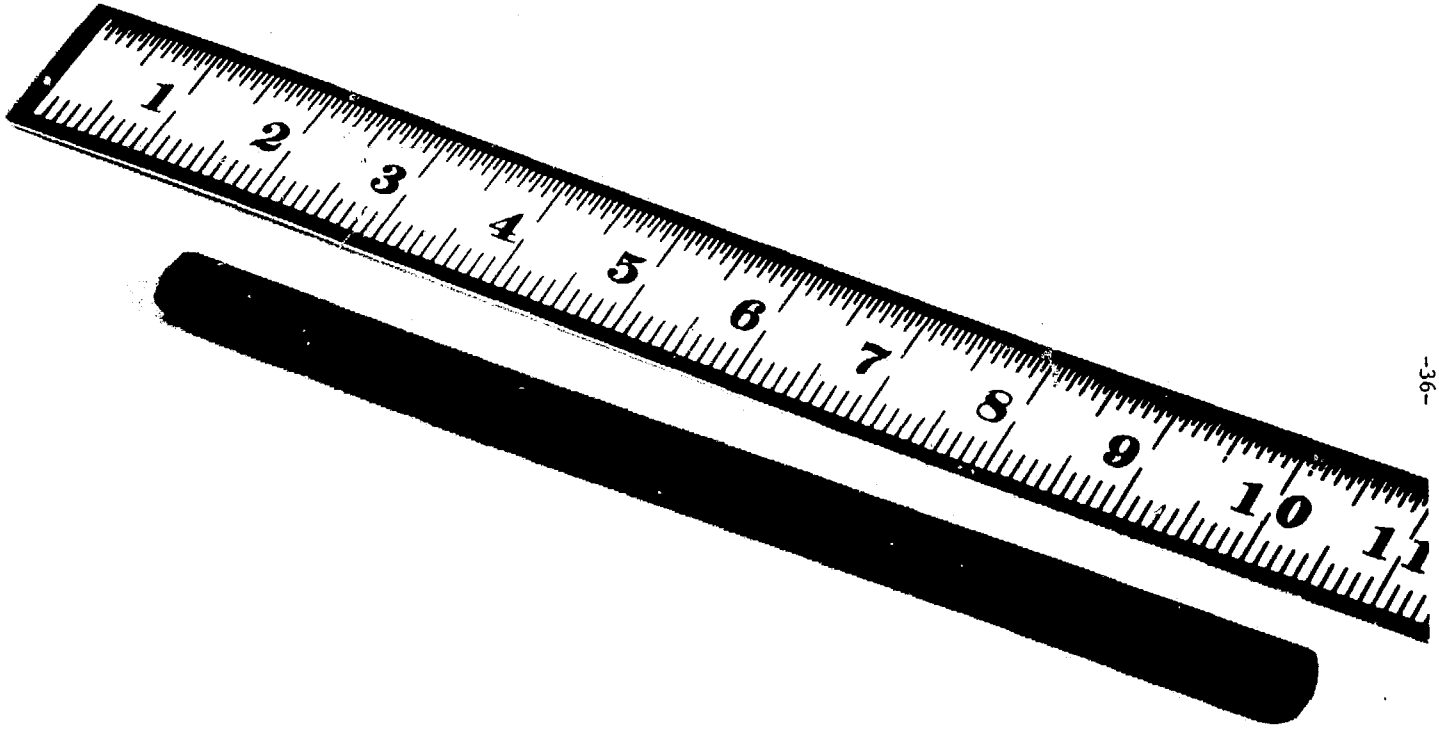

XBB 785-8333

Fig. 11.

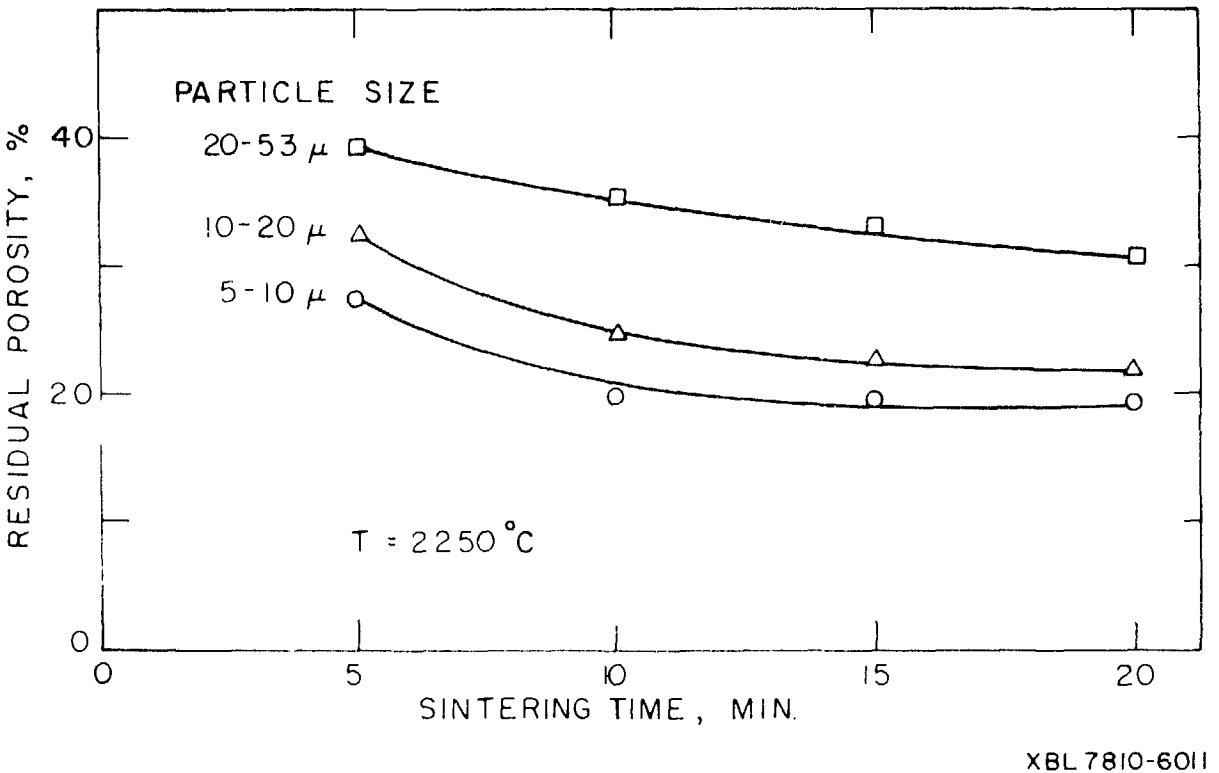
PARTICLE SIZE
20-53 μ
10-20 μ
5-10 μ
T = 2250 °C
RESIDUAL POROSITY, %
40
20
0
0
5
10
15
20
SINTERING TIME, MIN.
XBL 7810-6011

Fig. 14.

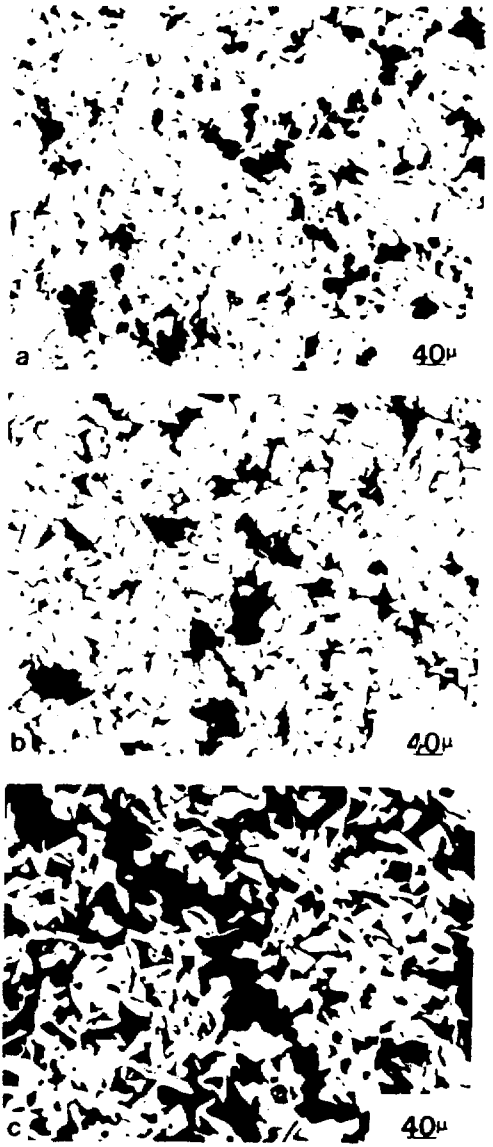

Fig. 15.

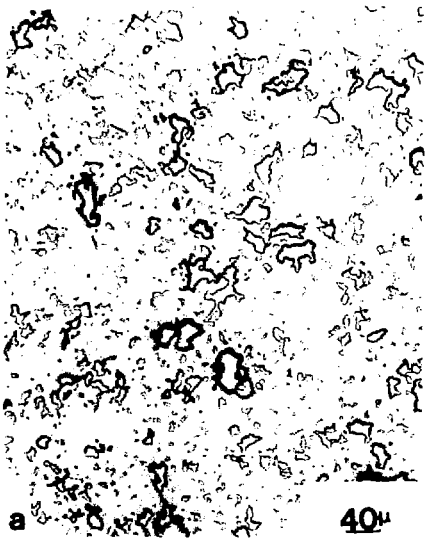

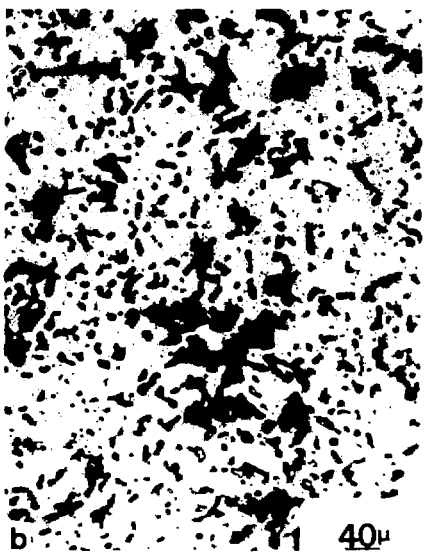

YBB 7910-13806

Fig. 16.

XBB 7810-13808

Fig. 17.

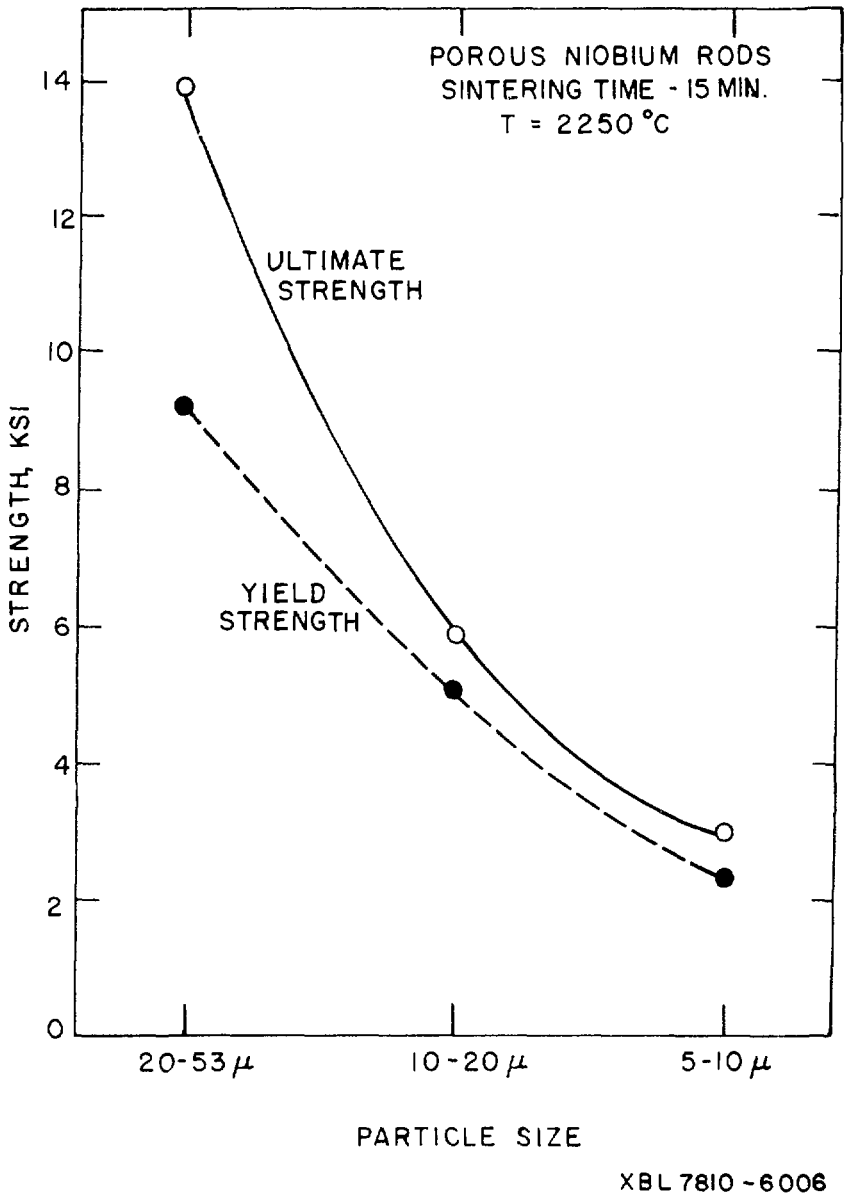
POROUS NIOBIUM RODS
SINTERING TIME - 15 MIN.
T = 2250 °C
ULTIMATE STRENGTH
YIELD STRENGTH
STRENGTH, KSI
0
2
4
6
8
10
12
14
20-53 μ
10-20 μ
5-10 μ
PARTICLE SIZE
XBL 7810-6006

Fig. 18.

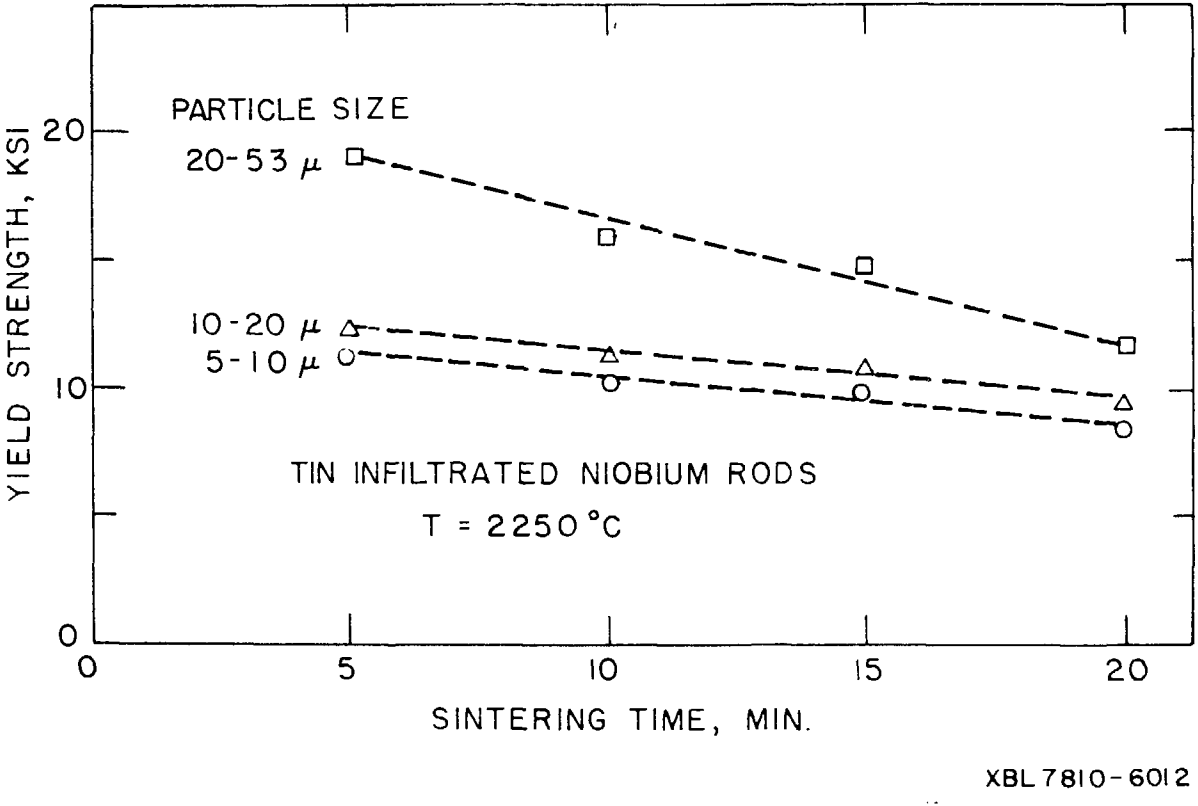
PARTICLE SIZE
20-53 μ
10-20 μ
5-10 μ
TIN INFILTRATED NIOBIUM RODS
T = 2250 °C
YIELD STRENGTH, KSI
SINTERING TIME, MIN.
0
10
20
0
5
10
15
20
XBL 7810-6012

Fig. 19.

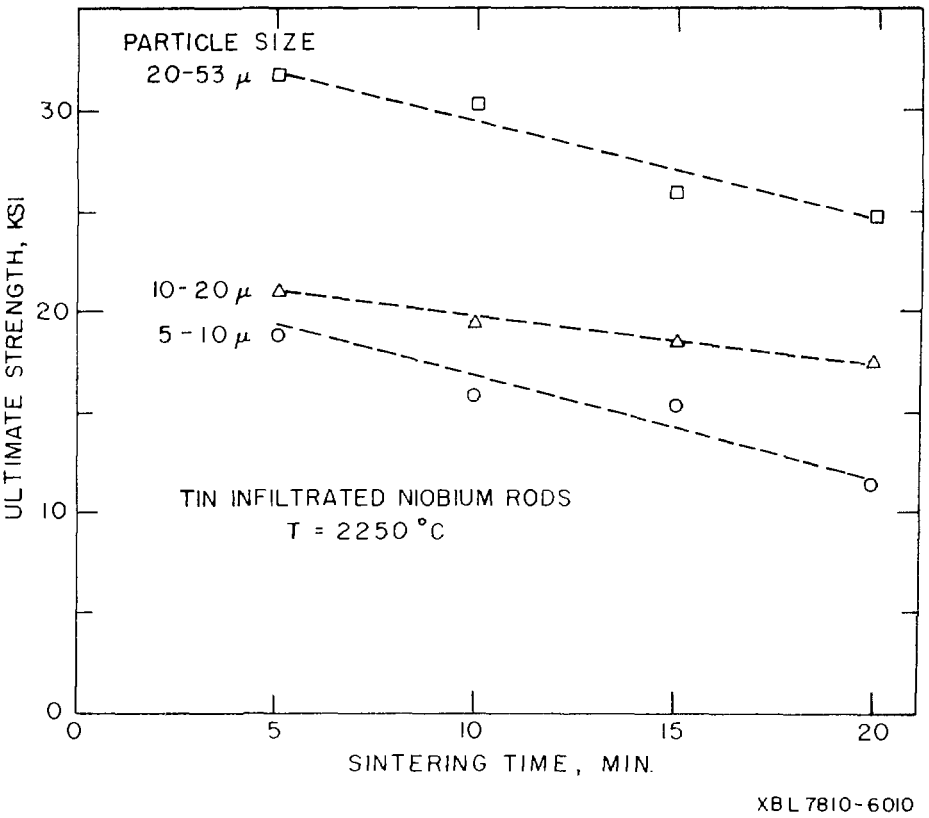
PARTICLE SIZE
20-53 μ
10-20 μ
5-10 μ
TIN INFILTRATED NIOBIUM RODS
T = 2250 °C
ULTIMATE STRENGTH, KSI
SINTERING TIME, MIN.
0
10
20
30
0
5
10
15
20
XBL 7810-6010

Fig. 20.

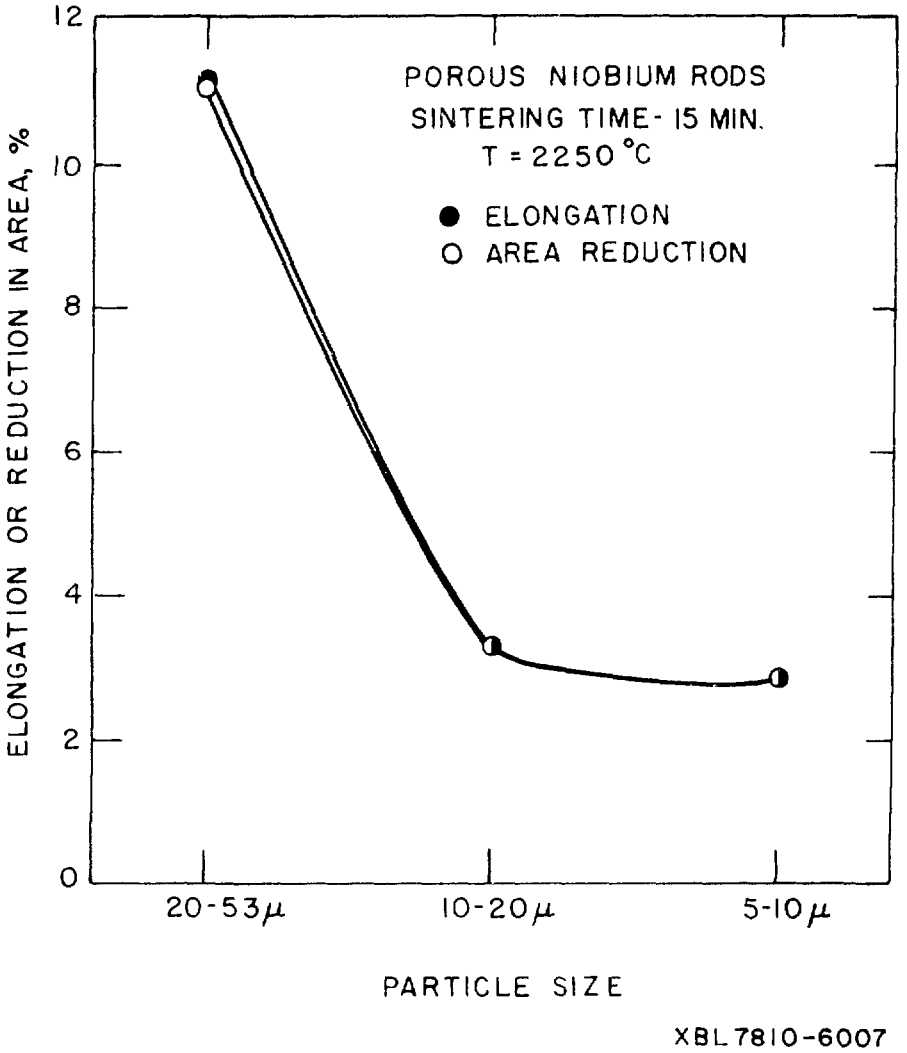
POROUS NIOBIUM RODS
SINTERING TIME- 15 MIN.
T = 2250 °C
ELONGATION
AREA REDUCTION
ELONGATION OR REDUCTION IN AREA, %
0
2
4
6
8
10
12
20-53μ
10-20μ
5-10μ
PARTICLE SIZE
XBL 7810-6007

Fig. 21.

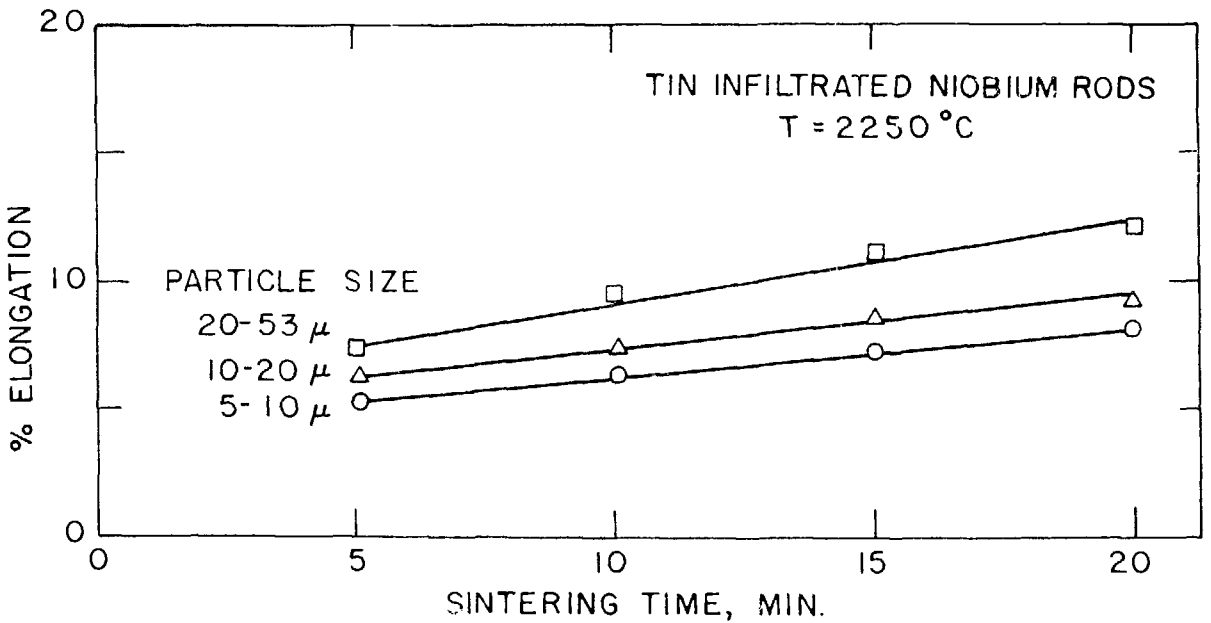

XBL 7810-6013

Fig. 22.

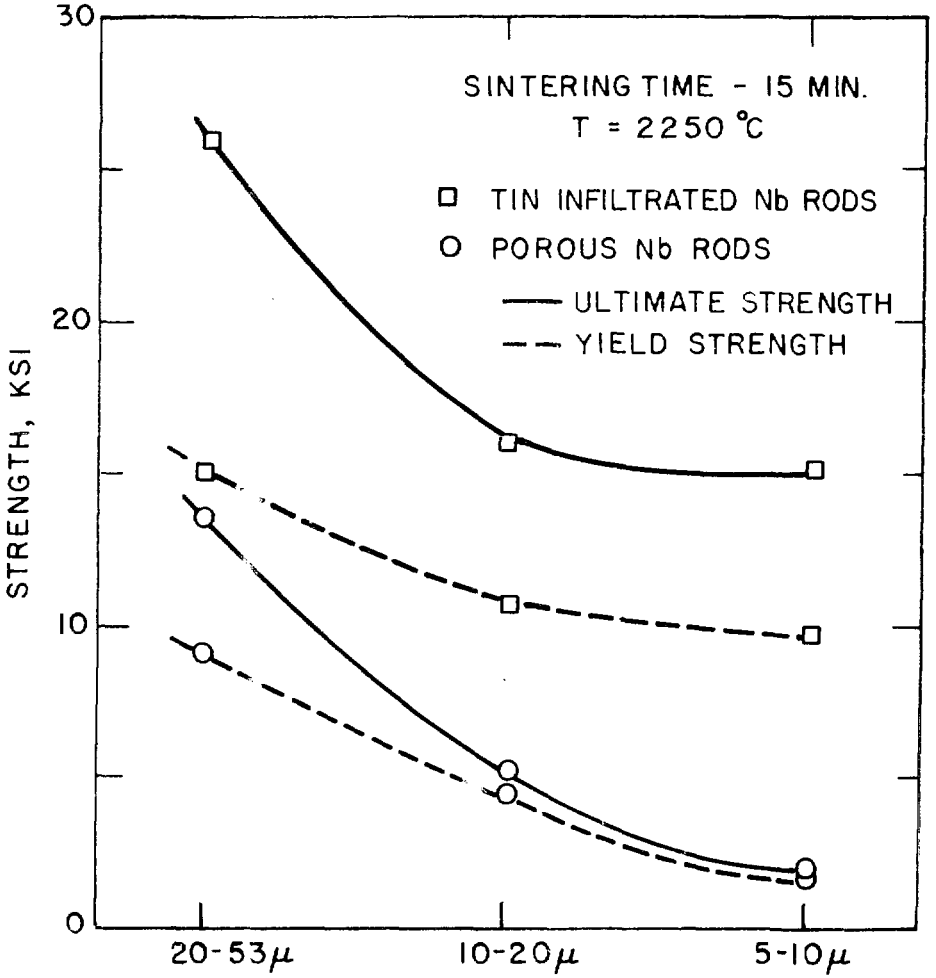

XBL7810-6004

Fig. 23

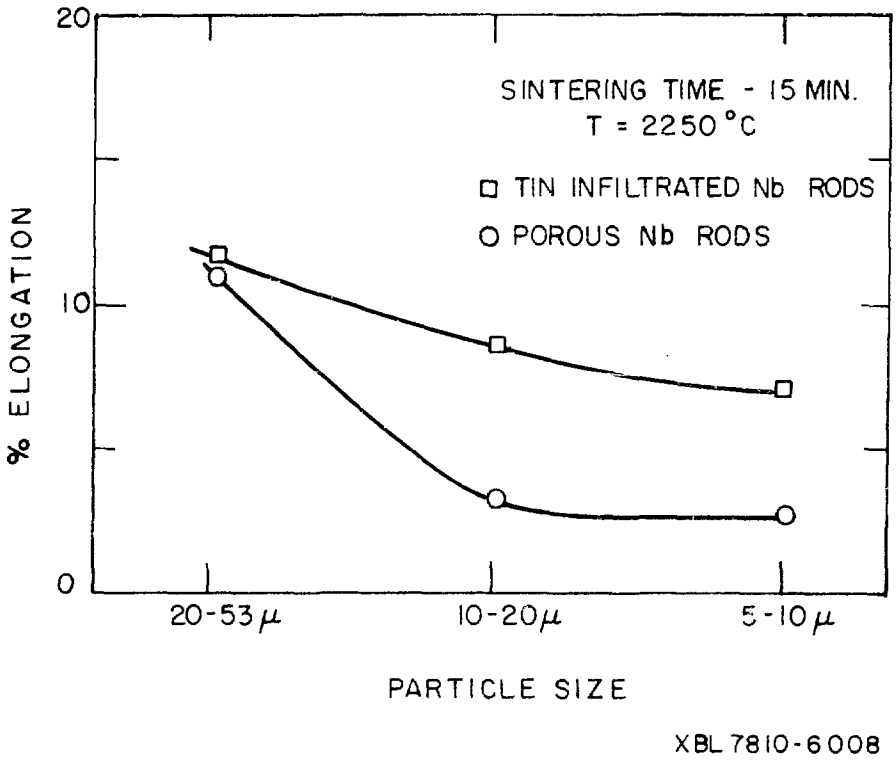
20
10
0
% ELONGATION
SINTERING TIME - 15 MIN.
T = 2250 °C
□ TIN INFILTRATED Nb RODS
○ POROUS Nb RODS
20-53 μ
10-20 μ
5-10 μ
PARTICLE SIZE
XBL 7810-6008

Fig. 24.


a
10μ

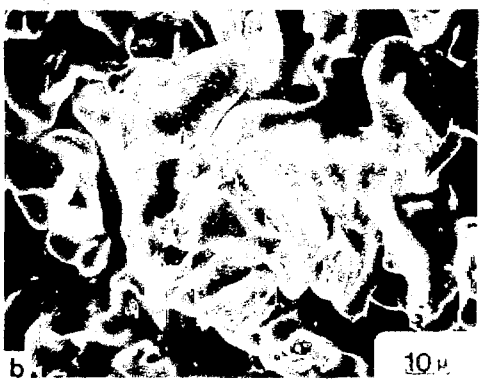
b
10μ

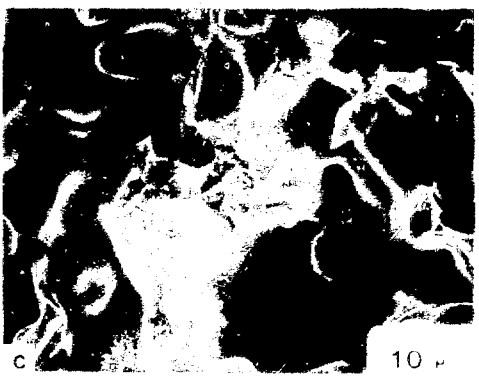
c
10 μ


a
10 μ


b
10μ

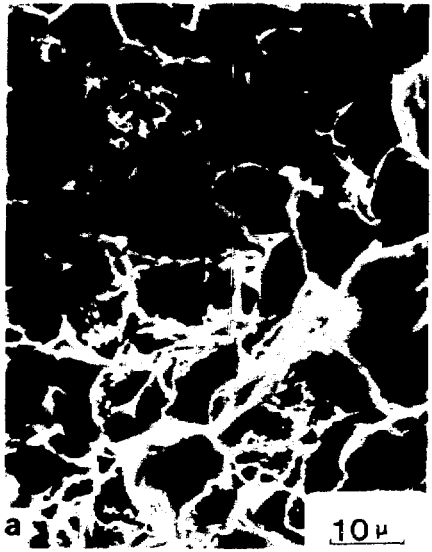
a
10 μ


b
10 μ